Controlled frustration in the antiferromagnetic triangular lattice $LiNi_{1-x}Co_xO_2$ (0<or=x<or=1)

1992 J. Phys.: Condens. Matter 4 6291

(http://iopscience.iop.org/0953-8984/4/29/013)

J. Phys.: Condens. Matter 4 (1992) 6291–6302. Printed in the UK

Controlled frustration in the antiferromagnetic triangular lattice $LiNi_{1-x}Co_xO_2$ ($0 \leqslant x \leqslant 1$)

K Hirota, H Yoshizawa and M Ishikawa
Institute for Solid State Physics, University of Tokyo, Minato-ku, Tokyo 106, Japan

Received 30 December 1991, in final form 19 March 1992

Abstract. In order to study the effects of frustration on the magnetic properties of the antiferromagnetic triangular lattice $LiNi_{1-x}Co_xO_2$, we measured the temperature dependence of both the magnetization and the AC susceptibility. With a random substitution of non-magnetic Co ions for Ni ions, the characteristic temperatures T_{N1} ($\simeq 240$ K) and T_{N2} ($\simeq 35$ K) gradually shifted to higher and lower temperatures, respectively, and the magnetic moment per Ni ion was drastically enhanced between T_{N1} and T_{N2}. The spin angular momentum of the Ni^{3+} ion, however, remains at about 0.5, confirming the low-spin state over the whole range of concentrations. We also performed neutron-scattering experiments and found that the intensity of diffuse scattering in the forward directions at low temperatures decreases on substitution. A new model for the magnetic interactions in $LiNiO_2$ is proposed on the basis of these results.

1. Introduction

The crystal structure of $LiNiO_2$ is called the α-$NaFeO_2$ type, which has a rhombohedral $R\bar{3}m$ symmetry [1]. This is a modified NaCl structure in which close-packed triangular lattices of each kind of atom are stacked in layer order Ni, O, Li, O and Ni with ABC stacking. The magnetic properties of $LiNiO_2$ are summarized as follows.

(i) *Successive changes in the magnetization process.* Magnetic susceptibility measurements [2, 3] and ESR measurements [4] showed that the compound exhibits successive changes in the magnetization process at $T_{N1} \simeq 240$ K and $T_{N2} \simeq 35$ K. The AC susceptibility [3] showed a huge peak at T_{N2}, which shifts to lower temperatures with a refinement of the sample quality. The possibility of another characteristic temperature $T_{N3} \simeq 70$ K has been suggested [3].

(ii) *No long-range order.* Specific heat results [3] revealed that the magnetic entropy gradually decreases down to 0.4 K without any pronounced anomalies corresponding to long-range order. By neutron-scattering measurements [1, 5], no magnetic Bragg peaks have been confirmed between 1.4 and 300 K.

(iii) *Spin angular momentum $S = \frac{1}{2}$ ($g = 2.1$).* The ESR measurements suggested that the g-value is 2.1. The temperature dependence of the magnetization follows the Curie–Weiss law with $S = \frac{1}{2}$ above T_{N1}. The magnetization is saturated to $1.0\mu_B$ per Ni atom above 40 T at 4.2 K [6] and the magnetic entropy approaches $R \ln 2$ at around room temperature [3].

(iv) *Ferromagnetic correlations.* Neutron-scattering measurements [5] revealed a development of ferromagnetic short-range correlations in the forward direction below

0953-8984/92/296291+12$04.50

T_{N1} and a clear divergence at T_{N2}. ^{7}Li NMR experiments [7] detected a small internal field of 3.6 kOe at 4.2 K.

(v) *Spin-frozen state.* A relaxation phenomenon with a long time constant below T_{N2} was found in the response of the magnetization to abruptly changed fields [3]. The temperature dependence of the intensity of the neutron diffuse scattering [5] suggested a frozen spin pattern similar to a spin-glass phase below T_{N2}.

As for the electronic state of the Ni ion, several models have been proposed to explain some particular experimental results [2, 3, 8, 9]. In our previous work [3], we have shown that the Ni^{3+} low-spin state with an $S = \frac{1}{2}$ spin is consistent with all the results mentioned above and have conjectured that these properties can be understood in terms of the frustration on the antiferromagnetic triangular lattice. The frustration prevents magnetic moments from ordering spontaneously or in external fields. In general, the influences of frustration manifest themselves as successive magnetic transitions, a decrease in transition temperature or a disappearance of long-range order; they have, in fact, been revealed in $LiNiO_2$ as well as in other well known compounds such as $CsCoCl_3$ [10].

In order to clarify the precise nature of frustrated spin systems, it is desirable to control the strength of the frustration at will. Since the frustration is evoked on a subtle balance of interactions among spins, it is supposed to be very sensitive to imperfections on the triangular lattice. Thus, the frustration can be controlled by deliberately disturbing the lattice. We recently realized that it should be possible to control the strength of the frustration by substituting non-magnetic Co ions for Ni ions in $LiNiO_2$. The crystal structure of $LiNi_{1-x}Co_xO_2$ remains the same over the entire concentration range. Measurements of the specific heat, the resistivity and the susceptibility showed [11] that the end compound, $LiCoO_2$, is a semiconductor ($E_{gap} \simeq 0.06$ eV at 200 K) and a van Vleck paramagnet of Co^{3+} ions in the low-spin state. It would be interesting to know how the frustration affects the magnetic behaviour between $LiNiO_2$ and the van Vleck paramagnetism of $LiCoO_2$. We measured the temperature dependence of the magnetization with a SQUID susceptometer for sintered samples of $LiNi_{1-x}Co_xO_2$ ($0.0 \leqslant x \leqslant 1.0$) as well as the AC susceptibility. Neutron-scattering experiments were also performed in order to investigate spin correlations. We measured the temperature dependence of both powder profiles and forward scatterings for several samples with $x < 0.40$.

2. Experimental details

2.1. Sample preparation

We prepared sintered samples according to the method of Thomas *et al* [12]. Powders of Li_2O_2, NiO and CoO in the proper proportions were ground in a glove-box filled with dried argon and then pelletized. The pellets were heated to 850 °C very slowly under a stream of pure dried oxygen and maintained for 36 h before cooling to room temperature very slowly. This heating routine was repeated after regrinding. We prepared samples with $x = 0.00$, 0.025, 0.05, 0.10, 0.15, 0.20, 0.25, 0.40, 0.60, 0.80, 0.90, 0.95 and 1.00.

X-ray diffraction patterns indicated no peaks of foreign phases for the samples prepared in this way. The dependences of the lattice parameters on Co concentration x are shown in figure 1. As shown therein, the lattice parameters change

almost linearly with the concentration of Co, indicating that Vegard's law is obeyed. These results imply that Co ions randomly substitute for Ni sites over the entire concentration range as expected. The comparison of c with a_H suggests that the two-dimensionality is increasingly strengthened towards $LiCoO_2$ because the c-value becomes longer relative to the a_H-value.

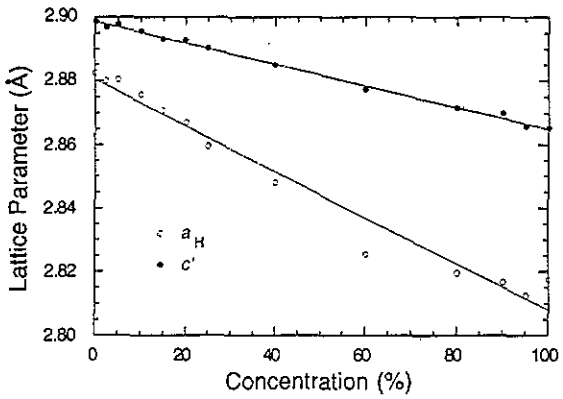

Figure 1. Variation in the lattice parameters a_H (○) and c' (●) in the conventional hexagonal unit cell with Co concentration x. c' is defined as $c' = c \times \sqrt{2}/4\sqrt{3}$ so that c' would coincide with a_H in the case of a perfect cubic closest packing.

For the present system, we tried to estimate the composition using the mass loss during a heat treatment. Thomas *et al* [12] suggested that LiOH, which exists as an impurity in the starting material Li_2O_2, has a significant vapour pressure above 800 °C. By assuming that the mass loss is caused only by the evaporation of LiOH, we estimated the composition of $LiNi_{1-x}Co_xO_2$.

For $x = 0.0\%$ (KH114 [3]), 2.9% of mass loss after the heat treatment is converted into a loss of 0.12 mol of LiOH per mole of $LiNiO_2$, which corresponds to $Li_{0.88}NiO_{1.88}$, i.e. the composition is $Li_{0.94}Ni_{1.06}O_2$. On the other hand, the composition is found to be $Li_{0.944}Ni_{1.056}O_2$ according to the relationship in [13] between the Li content and the cell volume, from which we estimated the composition of $LiNiO_2$ in our previous paper [3]. We also found that the compositions of several other $LiNiO_2$ samples estimated by these two methods agree very well within ±1% error. Therefore, we may conclude that monitoring the mass loss is another way of estimating the composition, although it is not a direct technique.

We applied this method to $LiNi_{1-x}Co_xO_2$ samples and found that the Li contents are 0.95 ± 0.02 for $0.0 \leqslant x \leqslant 0.8$ and 0.97 ± 0.01 for $0.8 \leqslant x \leqslant 1.0$. We also found that the Li content of $LiNi_{1-x}Co_xO_2$ strongly depends on the amount of LiOH in the starting material, Li_2O_2, as we previously reported for $LiNiO_2$ [3]. Finally, we comment that the amount of loss can be estimated from the ratio of the (1 0 4) peak intensity to the (0 0 3) peak intensity because the (0 0 3) peak is quite sensitive to the regularity of the ABC stacking of layers while the (1 0 4) peak is not. This analysis of peak intensities also showed no sign of considerable loss of Li.

The following should be noted about the profiles of the diffraction peaks. For the samples with $0.4 \leqslant x \leqslant 0.8$, the peaks except $(0\,0\,3n)$ broaden to almost twice the width of the $LiNiO_2$ peaks and become asymmetrical with a tail extending towards

smaller angles. The noticeable deviation of a_H from the straight line in figure 1 in this concentration range may be related to this broadening.

2.2. *Magnetization*

The magnetization M was measured with a SQUID magnetometer from 400 down to 6 K in a uniform magnetic field of 1 kOe. The results are shown as a function of temperature in figure 2. The magnetization M in the figure is given in units of μ_B per Ni^{3+} ion, where M was calculated by subtracting the magnetization for $LiCoO_2$ as the temperature-independent background (the van Vleck susceptibility was estimated to be 9.95×10^{-7} emu g^{-1} [11]):

$$M_{Ni^{3+}} = (M_{LiNi_{1-x}Co_xO_2} - xM_{LiCoO_2})/(1-x). \tag{1}$$

With increase in the Co concentration, $M_{Ni^{3+}}$ in the intermediate state ($T_{N1} > T > T_{N2}$) is drastically enhanced in the range $0.15 < x < 0.95$. Simultaneously, T_{N1} shifts gradually to a higher temperature. These results are shown more clearly in figure 3, in which figure 2 is replotted in a three-dimensional form. Furthermore, a valley centring along $x = 0.15$ and the abrupt change in the shape of the M versus T curve around $x \simeq 0.95$ are noteworthy.

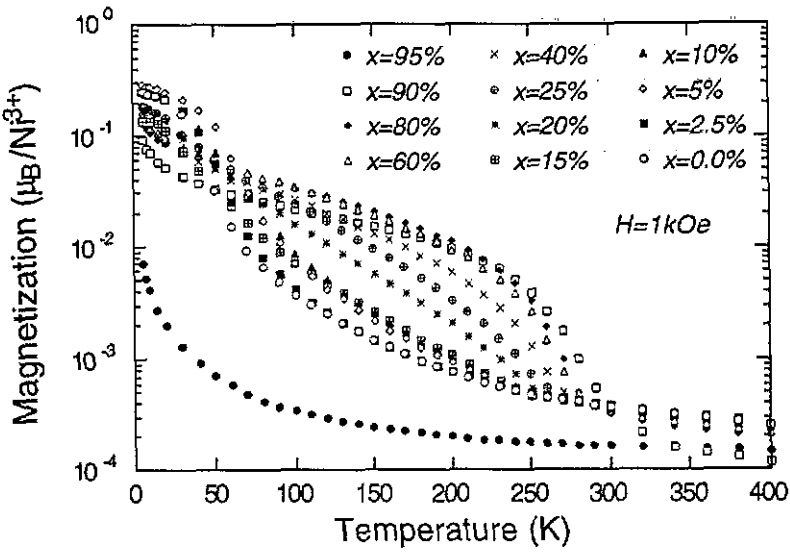

Figure 2. Temperature dependence of the magnetization per Ni^{3+} ion of $LiNi_{1-x}Co_xO_2$ for x-values of 0.00 (○), 0.025 (■), 0.05 (◇), 0.10 (▲), 0.15 (⊞), 0.20 (*), 0.25 (⊕), 0.40 (×), 0.60 (△), 0.80 (♦), 0.90 (□) and 0.95 (●) measured at 1 kOe.

We have defined T_{N1} as the temperature at which the inverse susceptibility $\chi_{DC}^{-1} = (M/H)^{-1}$ deviates from the Curie–Weiss law [3]. For a quantitative discussion of the relation between M and x, it is convenient to use the temperature as T_{N1} which gives the maximum of the temperature derivative dM^{-1}/dT of inverse magnetization. As

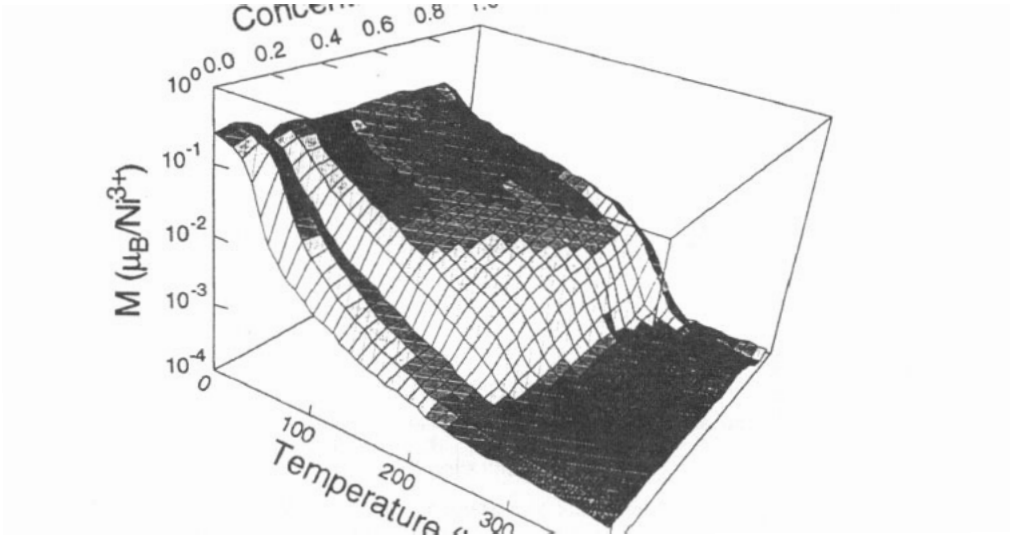

Figure 3. Temperature dependence of the magnetization per Ni^{3+} ion of $LiNi_{1-x}Co_xO_2$ measured at 1 kOe in three-dimensional form.

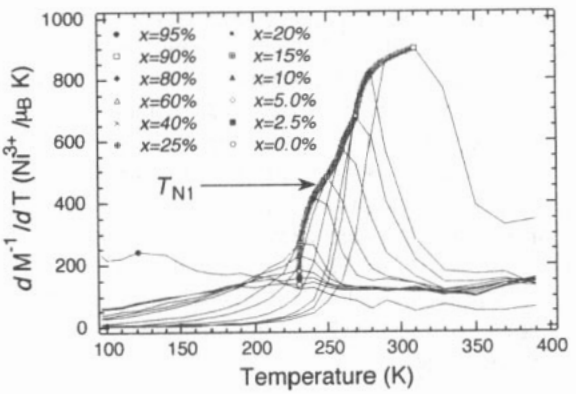

Figure 4. Variation in T_{N1} with x of $LiNi_{1-x}Co_xO_2$ for x-values of 0.00 (○), 0.025 (■), 0.05 (◇), 0.10 (▲), 0.15 (⊞), 0.20 (*), 0.25 (⊕), 0.40 (×), 0.60 (△), 0.80 (◆), 0.90 (□) and 0.95 (●). T_{N1} is defined as the temperature at which dM^{-1}/dT reaches a maximum.

shown in figure 4, T_{N1} monotonically increases from 230 K at $x \simeq 0.15$ up to the maximum value of 310 K at $x = 0.90$ and vanishes beyond $x = 0.90$.

To obtain the Curie constant for Ni^{3+} ions in the compound, we fitted the data with the Curie–Weiss law well above T_{N1}, where the inverse susceptibility attains an almost constant gradient. We estimated the spin quantum number S, provided that the orbital angular momentum L is frozen and that the g-value is equal to 2.1, which was obtained in the ESR measurements [4]. The S-values thus obtained are shown in

figure 5. It should be noted that S is almost 0.5 over the whole range. These facts favour our model of the $3d^7$ low-spin state for the spin state of the Ni ion.

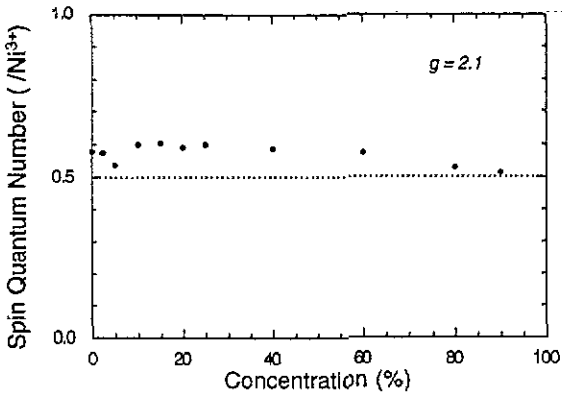

Figure 5. Variation in the spin quantum number per Ni^{3+} ion with x for $LiNi_{1-x}Co_xO_2$, which is obtained by fitting the inverse susceptibility with the Curie–Weiss law in the constant gradient range.

2.3. *AC susceptibility*

The AC susceptibility χ_{AC} was measured in an AC field of 100 mOe RMS at 123 Hz without static external fields. Thus, χ_{AC} probes the initial susceptibility. The results are shown in figure 6. The vertical axes of the figures represent the voltage of the secondary coil in microvolts normalized by the sample mass in grams.

The samples of low concentration demonstrate a huge peak, as shown in figure 6(*a*). The temperature where the peak is observed coincides with T_{N2} which is formerly defined from the M versus T curve [3]. Thus we redefine this temperature as T_{N2} for an easier and more precise determination. One can see that T_{N2} shifts to higher temperatures initially with substitution, reaching the maximum value of 50 K at $x = 0.05$, and then drops to lower temperatures. The rate of change in T_{N2} seems to slow down at around $x \simeq 0.20$. From $x = 0.40$ to $x = 0.80$, T_{N2} remains at around 4 K. Finally, T_{N2} diminishes below our low-temperature limit of 0.4 K for $x \geqslant 0.90$. On the other hand, we observed the upturn in χ_{AC} at low temperatures for $0.60 \leqslant x \leqslant 0.90$, as shown in figure 6(*b*).

2.4. *Neutron diffraction*

Neutron-scattering experiments were carried out on the triple-axis spectrometer ISSP-ND1 installed at JRR2, Japan Atomic Energy Research Institute, Tokai. The spectrometer was operated in the double-axis mode with an incident neutron momentum $k = 2.570$ Å^{-1}.

The sintered sample of $LiNi_{1-x}Co_xO_2$ ($x = 0.05$, 0.10, 0.20 and 0.40) was powdered in an agate mortar and then packed in a thin aluminium case (20 mm×20 mm×4 mm). The sample case was supported vertically in an aluminium can filled with He gas and mounted on a cold finger of a closed-cycle He-gas refrigerator in which the sample temperature is controllable to within 0.2 K between 17 and 300 K. No external fields were applied to the sample.

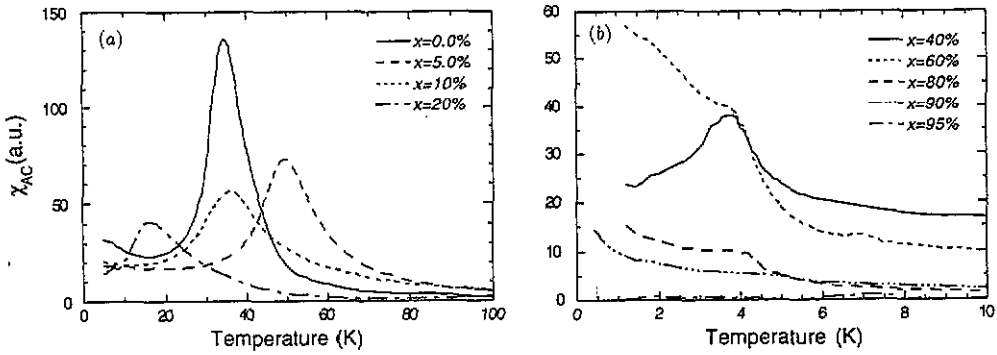

Figure 6. Temperature dependence of the AC susceptibility of $LiNi_{1-x}Co_xO_2$ for x-values of (*a*) 0.00 (——), 0.05 (– – –), 0.10 (- - -), 0.20 (— · —), (*b*) 0.40 (——), 0.60 (- - -), 0.80 (– – –), 0.90 (— · · —) and 0.95 (— · —) without external fields (a.u., arbitrary units). The vertical axis is normalized by the sample mass.

We first took powder profiles from $2\theta = 10°$ to $2\theta = 85°$ at 300, 200, 100 and 17 K. Relaxed collimations of 80′ and 40′ were used in front of and behind the sample, respectively. A pyrolytic graphite filter was placed in front of the sample to eliminate higher-order contaminations. As reported previously for $LiNiO_2$ [2, 5], no additional peaks other than the nuclear peaks were found in $LiNi_{1-x}Co_xO_2$. Moreover, no anomalous temperature dependences of the intensities of the nuclear peaks were detected. As for the (0 0 3) peak for $x = 0.40$, we investigated the profile in detail and estimated the temperature dependence of the integrated intensity by a least-squares fitting with the Gaussian. The results are shown in figure 7. It is expected that a ferromagnetic alignment of the spins of $1\mu_B$ would enhance the peak intensity by approximately 5%. The statistics of the measurements can detect the ferromagnetic polarization if it is larger than $0.5\mu_B$. However, we did not find such an enhancement of the peak intensity. This result is consistent with the temperature dependence of the magnetization and the previous neutron diffraction measurement [5]. Furthermore, we found no anomalies in particular around the characteristic temperature T_{N1} or around T_{N2}. The slight decrease in integrated intensity at low temperatures is due to an instrumental reason; thus, it should have no physical meaning.

We then studied the temperature dependence of the forward scattering, which represents short-range ferromagnetic correlations [5]. The scattering angles were kept fixed between 0.8° and 1.0°. We used collimations of 20′ and 20′ to reduce the background from the direct beam. The results are shown in figure 8, in which the data are normalized by the room-temperature value. No temperature dependences were observed for $x = 0.40$ and 0.20. However, the intensity for $x = 0.10$ shows an almost monotonic increase with decreasing temperature. The intensity at 15 K is about 12% larger than that at room temperature. The intensity for $x = 0.05$ exhibits a distinct increase below 100 K, reaching about 120% at 15 K. Nevertheless, we found no critical divergence as was observed for $LiNiO_2$ at T_{N2} [5].

3. Discussion and summary

3.1. Magnetic phase diagram

As shown in figures 2 and 3, the magnetization per Ni ion is enhanced on substitu-

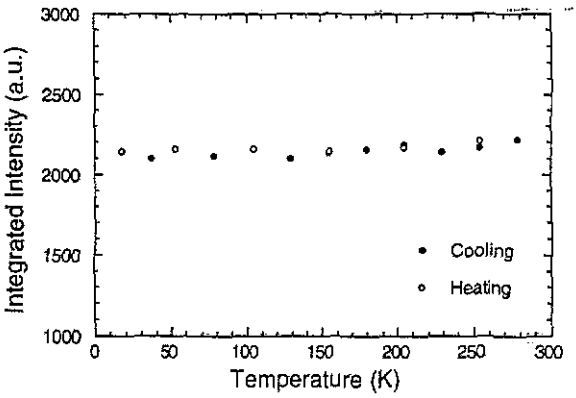

Figure 7. Temperature dependence of the integrated intensity of the (0 0 3) peak for $LiNi_{0.6}Co_{0.4}O_2$ on cooling (●) and heating (○).

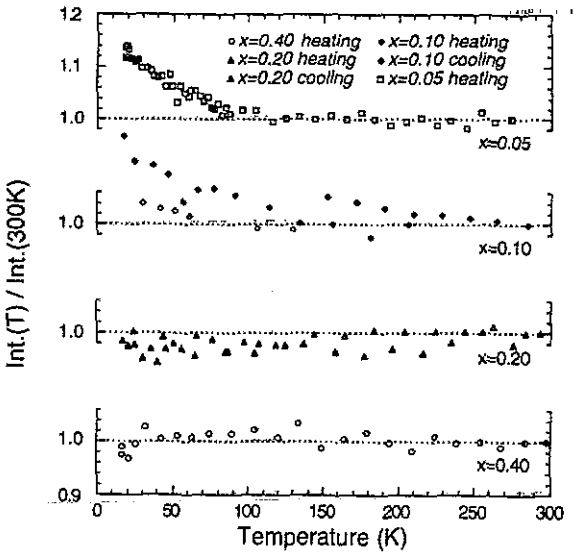

Figure 8. Temperature dependence of the forward-scattering intensity of $LiNi_{1-x}Co_xO_2$: □, $x = 0.05$, heating; ◆, $x = 0.10$, cooling; ◇, $x = 0.10$, heating; ▲, $x = 0.20$, cooling; △, $x = 0.20$, heating; ○, $x = 0.40$, heating. The intensities are normalized by the room-temperature value. The scattering angles were kept fixed at 0.8–1.0°.

tion of *non-magnetic* Co ions for magnetic Ni ions, particularly for $0.20 \leqslant x \leqslant 0.90$. There are two possible reasons for this enhancement of the magnetization: one is the decline in the frustration resulting from perturbing the triangular lattice symmetry, and the other is due to increased ferromagnetic interactions. However, the latter possibility can be rejected because the neutron-scattering experiments revealed the contrary, i.e. the forward-scattering intensity due to ferromagnetic correlations disappears on substitution. Therefore, it is most probable that this phenomenon can be ascribed to the partial release of the frustration. Before discussing interactions in $LiNi_{1-x}Co_xO_2$, we shall summarize the experimental results.

A magnetic phase diagram is proposed in figure 9. It is reasonable that T_{N1} shifts to higher temperatures on substitution because the frustration, which tends to depress transition temperatures, is released as the triangular lattice is disturbed by substitution. The variation in T_{N2} with Co concentration, on the other hand, seems to involve more complicated physics. The increase in T_{N2} below $x = 0.05$ may be interpreted as a similar effect of frustration as for T_{N1}. Beyond that concentration, however, it is necessary to take into account at least two different effects: the effect of depressed frustration and the effect of dilution on low-dimensional magnets. The latter was extensively studied by Stinchcombe [14]. For the case of a weakly coupled layer magnet with Ising anisotropy, as the magnetic concentration p is reduced (i.e. as the non-magnetic concentration x in our notation is increased) towards the two-dimensional percolation concentration $P_c^{(2)}$, the transition temperature T_c falls until $k_B T_c$ becomes comparable with the weak exchange between layers. This weak exchange raises the effective dimensionality to three so that the critical curve T_c versus p flattens off and heads towards the smaller limiting concentration $P_c^{(3)}$ for the three-dimensional system. This striking phenomenon is called 'dimensional crossover' in dilute magnets. Several critical curves were calculated for various ratios γ of interlayer coupling to intralayer coupling. The critical curve of T_{N2} for the present system is quite similar to that calculated for $\gamma = \frac{1}{10}-\frac{1}{50}$. This supports good two-dimensionality in $LiNiO_2$.

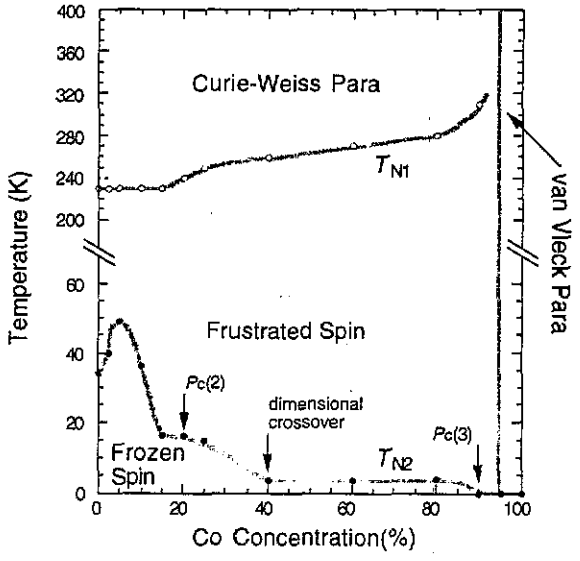

Figure 9. Magnetic phase diagram of $LiNi_{1-x}Co_xO_2$.

As mentioned in the preceding section, a spin-frozen state is realized below T_{N2} in $LiNiO_2$. In order to confirm that this state is also realized in $LiNi_{1-x}Co_xO_2$, we studied the time dependence of the magnetization for $x = 0.20$, 0.40 and 0.80. We found a logarithmic time dependence below T_{N2} as seen in $LiNiO_2$ [3]. It is well known that such a phenomenon is typical of spin-glass materials. Therefore, $LiNi_{1-x}Co_xO_2$ presumably forms a sort of spin-frozen phase below T_{N2}, although

the origin may vary depending on which concentration range we are concerned with. (See the T_{N2} curve in figure 9.)

3.2. Possible models of the magnetic structure of $LiNiO_2$

From the above discussion, it is concluded that $LiNiO_2$ is suitable for a model of a two-dimensional triangular lattice magnet with a weak interlayer coupling. It is also evident that $LiNiO_2$ has both antiferromagnetic correlations, which induce the frustration, and ferromagnetic correlations, as observed in the magnetic diffuse scattering in the forward direction. To reconcile these experimental results we consider the following model:

$$H = -2J_1 \sum_i \sum_{\mu\nu}^{NN} S_\mu^i S_\nu^i - 2J_2 \sum_i \sum_{\mu\nu}^{NNN} S_\mu^i S_\nu^i - 2J' \sum_i \sum_{\mu\nu}^{NN} S_\mu^i S_\nu^{i+1} - g\mu_B H \sum_i \sum_\mu S_{z\mu}^i \qquad (2)$$

where S_μ^i denotes the μth spin on the ith layer. The first term represents intralayer nearest-neighbour (NN) correlations, the second term intralayer next-nearest-neighbour (NNN) correlations and the third term interlayer nearest-neighbour correlations. We presume here that $J_1 < 0$ (antiferromagnetic), $J_2 < 0$ (antiferromagnetic), $J' > 0$ (ferromagnetic) and $|J_1| > |J_2| \gg |J'|$.

It is well known that a three-sublattice state is stable in the triangular lattice with $J_1 < 0$ and $J_2 > 0$ [15]. According to the mean-field approximation, there are two transition temperatures. The higher ordered state is called the partially disordered state, in which two sublattices are ordered antiferromagnetically while the other remains in disorder. The lower ordered state is the ferrimagnetic (*up–up–down*) state. The three-sublattice state exhibits a one-third plateau on M versus H curves and magnetic Bragg peaks at $(\frac{1}{3}\ \frac{1}{3}\ n)$ in neutron diffraction. These two phenomena are observed in many quasi-one-dimensional [10] and several two-dimensional antiferromagnetic triangular lattices [16], while neither has been confirmed in $LiNiO_2$.

Although the above model has not been studied as thoroughly as other theoretical models for the antiferromagnetic triangular lattice [15, 17, 18], this model seems to have two distinct features: firstly, the three-sublattice state is unstable and, secondly, the frustration among nearest neighbours through J_1 is partially cancelled by the frustration among next-nearest neighbours through J_2. Because of the latter, the ferromagnetic exchange J', even though it is small, will have a substantial influence on the magnetic behaviour at low temperatures and the external field necessary for saturating the magnetization at low temperatures becomes lower than that expected from J_1. Moreover, the magnetization saturates without showing the one-third plateau because the ferrimagnetic state is unstable even in high fields.

In a triangular lattice $CuFeO_2$ [19] and a Kagomé lattice $SrCr_{8-x}Ga_{4+x}O_{19}$ [20], two-dimensional magnetic short-range order and an incommensurate spin structure were recently discovered. However, no definite experimental evidence for antiferromagnetic correlations has been obtained for $LiNiO_2$ yet, although antiferromagnetic correlations are a prerequisite for the frustration under consideration. The resonating-valence-bond state (quantum fluctuations) [21] or short-range order with multiple incommensurate wavevectors [18] may be realized for $LiNiO_2$, both of which

would make an experimental confirmation of spin structure difficult. It would be, in any case, very important to ascertain in what form antiferromagnetic correlations manifest themselves for $LiNiO_2$.

4. Conclusions

The magnetization, AC susceptibility and neutron diffraction of the triangular lattice magnet $LiNi_{1-x}Co_xO_2$ have been measured. We have shown the novel effect of dilution on the enhancement of the magnetic moment and T_{N1}. These observations corroborate the existence of frustration, which we had conjectured to explain the magnetic properties of $LiNiO_2$ [3]. The unusual dependence of T_{N2} on the dilution has been successfully rationalized by the frustration and the dimensional crossover in dilute magnets. Comparison with the theory of dilute magnets proposed by Stinchcombe [14] suggests that the interlayer coupling in the present system is in fact weak.

On the basis of the experimental results obtained so far, we have introduced a new model which consists of antiferromagnetic intralayer NN and NNN couplings and a weak ferromagnetic interlayer coupling. One of the most distinct features about this model is the instability of the three-sublattice state, which is consistent with the lack of both the one-third plateau on the magnetization curves and the magnetic Bragg peaks at $(\frac{1}{3}\ \frac{1}{3}\ n)$.

Acknowledgments

We are grateful to Professor F Matsubara and Professor S Miyashita for valuable discussions about the magnetic structure of $LiNiO_2$. We would like to thank Dr P Kuiper for communicating his result from XAS measurements. We are especially indebted to Dr Y Nakazawa for pointing out the possibility of the non-magnetic state of Co^{3+}.

References

[1] Dyer L D, Borie B S Jr and Smith G P 1954 *J. Am. Chem. Soc.* **20** 1499
[2] Hirakawa K, Kadowaki H and Ubukoshi K 1985 *J. Phys. Soc. Japan* **54** 3526
[3] Hirota K, Nakazawa Y and Ishikawa M 1991 *J. Phys.: Condens. Matter* **3** 4721
[4] Yamada I, Ubukoshi K and Hirakawa K 1985 *J. Phys. Soc. Japan* **54** 3571
[5] Yoshizawa H, Mori H, Hirota K and Ishikawa M 1990 *J. Phys. Soc. Japan* **59** 2631
[6] Goto T, Ariga H and Sakakibara T 1990 private communication
[7] Itoh M, Yamada I, Ubukoshi K, Hirakawa K and Yasuoka H 1986 *J. Phys. Soc. Japan* **55** 2125
[8] Kuiper P, Kruizinga G, Ghijsen J, Sawatzky G A and Verweij H 1989 *Phys. Rev. Lett.* **62** 221
[9] Kemp J P, Cox P A and Hodby J W 1990 *J. Phys.: Condens. Matter* **2** 6699
Kemp J P and Cox P A 1990 *J. Phys.: Condens. Matter* **2** 9653
[10] Mekata M and Adachi K 1978 *J. Phys. Soc. Japan* **44** 806
[11] Hirota K 1990 *MSc Thesis* University of Tokyo (in Japanese)
[12] Thomas M G S R, David W I F and Goodenough J B 1985 *Mater. Res. Bull.* **20** 1137
[13] Goodenough J B, Wickham D G and Croft W J 1958 *J. Phys. Chem. Solids* **5** 107
[14] Stinchcombe R B 1980 *J. Phys. C: Solid State Phys.* **13** 5565
[15] Mekata M 1977 *J. Phys. Soc. Japan* **42** 76
[16] Sugihara T, Siratori K, Kimizuka N, Iida J, Hirayoshi H and Nakagawa Y 1985 *J. Phys. Soc. Japan* **54** 1139

[17] Miyashita S and Kawamura H 1985 *J. Phys. Soc. Japan* **54** 3385
[18] Matsubara F and Inawashiro S 1986 *J. Phys. Soc. Japan* **55** 1438; 1986 *Prog. Theor. Phys. Suppl.* **87** 77; 1987 *J. Phys. Soc. Japan* **56** 4087
[19] Mitsuda S, Yoshizawa H, Yaguchi N and Mekata M 1991 *J. Phys. Soc. Japan* **60** 1885
[20] Broholm C, Aeppli G, Espinosa G P and Cooper A S 1991 *J. Appl. Phys.* **69** 4968
[21] Fazekas P and Anderson P W 1974 *Phil. Mag.* **30** 423